APL Photonics

RESEARCH ARTICLE | JUNE 18 2024

Highly efficient lead zirconate titanate ring modulator

Guolei Liu ; Hongyan Yu ; Dasai Ban ; Bin Li ; Guoqiang Wei ; Chen Yang; Jungan Wang ; Young-Ik Sohn ; Yu Han; Feng Qiu

APL Photonics 9, 066111 (2024)
https://doi.org/10.1063/5.0193922

APL Photonics ARTICLE pubs.aip.org/aip/app

Highly efficient lead zirconate titanate ring modulator

Cite as: APL Photon. 9, 066111 (2024); doi: 10.1063/5.0193922
Submitted: 24 December 2023 • Accepted: 24 May 2024 •
Published Online: 18 June 2024

Guolei Liu,[1,2,3] Hongyan Yu,[4,5,a)] Dasai Ban,[2,3] Bin Li,[4,5] Guoqiang Wei,[4] Chen Yang,[4] Jungan Wang,[4] Young-Ik Sohn,[6] Yu Han,[7,b)] and Feng Qiu[4,a)]

AFFILIATIONS

[1] Zhejiang University, Hangzhou 310058, Zhejiang Province, China
[2] Key Laboratory of 3D Micro/Nano Fabrication and Characterization of Zhejiang Province, School of Engineering, Westlake University, Hangzhou 310024, Zhejiang Province, China
[3] Institute of Advanced Technology, Westlake Institute for Advanced Study, Hangzhou 310024, Zhejiang Province, China
[4] Hangzhou Institute for Advanced Study, University of Chinese Academy of Sciences, Hangzhou 310024, Zhejiang Province, China
[5] Shanghai Institute of Technical Physics, Chinese Academy of Sciences, Shanghai 200083, China
[6] School of Electrical Engineering, Korea Advanced Institute of Science and Technology (KAIST), Daejeon 34141, Republic of Korea
[7] Juhe Electro-optic (Hangzhou) Tech. Co., Ltd., Hangzhou 310024, Zhejiang Province, China

[a)] Authors to whom correspondence should be addressed: yuhongyan@ucas.ac.cn and A-photonics@outlook.com
[b)] Electronic mail: hanyutree@yahoo.co.jp

ABSTRACT

Advanced photonic integrated circuits require large-scale integration of high-speed electro-optic (EO) functional components on a chip. Low power consumption and high operation speed are thus key metrics for almost all integrated EO devices. Here, we demonstrated a ring resonator modulator based on lead zirconate titanate (PZT) on a SiO_2/Si substrate. The ridge waveguides were employed to keep a large spatial overlap between the optical field and the electric field within the PZT layer. The device exhibits a data rate of 56 Gbit/s and significant tuning efficiency, reaching up to 35.8 pm/V, corresponding to 1.17 V·cm. The demonstration of energy efficient and high-speed EO modulation paves the way for realizing dense PZT photonics integrated circuits.

I. INTRODUCTION

Global data traffic has witnessed an exponential increase with the fast development of 5G/B5G, artificial intelligence, cloud computing, and Internet of things.[1,2] Optical interconnection is a promising option to overcome transmission bottlenecks in data centers and high-performance computers. In the optical interconnection, an electro-optic (EO) modulator is a vital component that plays an information encoding engine from electrical to optical domain to ensure a high-speed data transmission.[3] Two types of EO modulators are most intensively studied: Mach–Zehnder interferometer (MZI) modulators and ring resonator modulators.[4–7] Compared to MZI, the advantages of ring modulators are their compact footprint, low driving voltage, and the ability to drive them as lumped RF elements that removes the need for traveling-wave design. Moreover, their wavelength selectivity enables dense wavelength division multiplexed links at the micrometer scale and consequently increases aggregate link bandwidth drastically.[8–10]

Up until now, ring modulators have been realized by using a number of material platforms, such as silicon (Si), EO polymer, and crystals.[11–13] Recent progress of Si modulators relying on the free-carrier plasma-effect is of interest and offers a realistic means of achieving ultra-fast data transfer, enabled by a careful balance among the doping configuration, loss control, and free-carriers' lifetime.[14] EO polymer benefiting from the strong Pockels effect with a high EO coefficient r_{33} > 100 pm/V can achieve outstanding linear modulation and low power-consumption.[15] However, the thermal and chemical stability of organic materials still needs to be validated. "EO ferroelectric thin-film on insulator" has emerged recently as a new candidate for the next generation of high-speed optical interconnect devices.[7,16–18] In this platform, a sub-micrometer-thick ferroelectric thin-film also with the Pockels effect is preferably bonded on top of a low-index SiO_2 substrate, and the waveguides are created by dry etching of the ferroelectric thin-film. This platform allows for an integration of photonic devices and high-speed electronic circuits, simultaneously enabling strong modal confinement and effective overlap between optics and electric signals.[19] Lithium niobate (LN) or barium titanate (BTO) thin-film ring modulators have been proven as an effective path to realize strong EO modulation within integrated photonics. For example, a high speed of 40 Gbit/s and a low $V_\pi L$ of 2.2 V·cm have been achieved in the LN ring modulator[13] and 40 Gbit/s and 0.45 V·cm in BTO racetrack resonator modulators.[20] Yet, these ring structures remain non-ideal due to relatively low EO tunability or high propagation loss. Caused by the relatively low EO coefficient as 30 pm/V, the EO tunability (defined as $\Delta\lambda_i/\Delta V$, where $\Delta\lambda_i$ is the resonance peak shift and V is the applied DC voltage) of the LN ring modulators is <10 pm/V.[21,22] Although BTO has a high EO coefficient, the high waveguide propagation loss ~10 dB/cm is still a major issue.[20,23] In addition, there are other concerns regarding the requirement of complex bonding fabrication of LN and BTO thin-films.

Lead zirconate titanate $PbZr_xTi_{1-x}O_3$ (PZT) thin-film is another promising candidate for EO modulators because of many desirable characteristics, such as a high EO coefficient, excellent optical transparency, and a straightforward chemical solution deposition (CSD) fabrication process.[24] PZT thin-film on silicon nitride (SiN) ring modulator has been realized with a data rate up to 40 Gbit/s and a low propagation loss of 1 dB/cm.[17] Despite this progress, some properties need to be improved further for the widespread utilization of the PZT modulators. These include a $V_\pi L$ of 3.2 V·cm, a relatively low in-device EO coefficient of 60 pm/V, and an estimated extinction ratio of merely ~1 dB at 40 Gbit/s modulation. Recently, we have explored "PZT ferroelectric thin-film on insulator (PZTOI)" and realized low propagation loss waveguides via the traditional photolithography and inductively coupled plasma (ICP) etching.[25] The obtained EO coefficient of the PZTOI is ~100 pm/V at the wavelength of 1550 nm, which leads to the decrease of $V_\pi L$ and the improvement of high-speed modulating quality. Furthermore, the refractive index contrast between PZT and SiO_2 is around 1.0. Such a large contrast may contribute to a small bending radius, which allows for a compact ring resonator and denser photonic circuit layout.

In this work, we have achieved high tuning efficiency and high-speed ring modulators on the PZTOI platform. The PZT thin film was fabricated by the chemical solution method on a SiO_2/Si substrate. The thin films can be directly deposited on substrates with high quality and low cost. The designed structure not only confines optical mode tightly in the PZT waveguide core but also effectively shorten the inter-electrode gap. The fabricated device is amenable to achieve a high EO effect, demonstrating a record high EO coefficient of 100 pm/V. The ring modulator shows an EO tunability of $\Delta\lambda_i/\Delta V$ = 35.8 pm/V, corresponding to $V_\pi L$ = 1.17 V·cm. A high-speed test of the modulator reveals an on–off keying (OOK) modulation up to 56 Gbit/s with an extinction ratio of ~3.1 dB.

II. DEVICE DESIGN AND FABRICATION

The structures of the ring modulator are shown in Figs. 1(a) and 1(b), where the waveguide consists of SiO_2 claddings, a PZT layer, aluminum (Al) co-planar electrodes, and a Si substrate. The refractive indices of SiO_2 and PZT are 1.45 and 2.40 at the wavelength of 1.55 μm, respectively. The thicknesses of top and bottom SiO_2 claddings are around 1.0 and 2.0 μm, respectively. The PZT ridge is totally 350 nm thick with a rib width of 1.0 μm for the single mode operation. For optimizing the device performance, the etching depth (d_e) and inter-electrode gap (g_{inter}) are carefully determined. Figure 1(b) shows the simulated optical TE mode-field and DC electric-field distribution in the device, indicating the large overlap between the optical and DC fields. Compared to previous ring modulator[17] on the PZT platform, a thicker PZT thin film can be fabricated on the SiO_2/Si substrate, and the ridge waveguide can distribute more light within the PZT layer. 80.9% of the optical field is distributed in the PZT layer, while 7.1% is found in the substrate and 12% is found in the top cladding layer. Therefore, a higher tuning efficiency and a high extinction ratio are achievable.

The EO tunability $\Delta\lambda_i/\Delta V = \Delta n_{pzt} \cdot L/\Delta V$ (L is the length of the electrode, 281 μm) is attributed to the PZT refractive index change (Δn_{pzt}), which corresponds to the in-device EO response of the ring resonator.[5,17] Theoretically expected Δn_{pzt} can be expressed as

$$\Delta n_{pzt} = \frac{1}{2} n_{pzt}^3 r \frac{\Delta V}{g_{inter}} \Gamma, \tag{1}$$

$$\Gamma = \frac{g_{inter}}{V} \frac{\varepsilon_0 c n_{pzt} \iint_{pzt} E_x^e \left|E_x^{op}\right|^2 dxdy}{\iint Re(\boldsymbol{E}^{OP} \times \boldsymbol{H}^{OP*}) \cdot \widehat{e_z} dxdy}, \tag{2}$$

where n_{pzt} is the PZT refractive index, r is the PZT in-device EO coefficient (estimated 130 pm/V[24]), V is the voltage, Γ is the EO overlap factor, $\varepsilon_0$is the vacuum permittivity, and c is the speed of light in vacuum. E_x^e is the in-plane (x direction) component of the electric field, and E_x^{op} represents the in-plane (x direction) transversal component of the optical field. According to Eq. (1), narrow-gap electrodes are beneficial to achieve a high $\Delta\lambda_i/\Delta V$. In addition, as shown in Fig. 1(c), a shallow etching depth (smaller d_e) is preferred to concentrate the optical mode in the active PZT core as much as possible (higher overlap factor). Meanwhile, a smaller d_e will inevitably cause a high absorption loss α_{abs} from the narrow-gap co-planar electrodes due to limited confinement of the optical mode. The Q factor of the ring resonator is determined by the waveguide loss. The device 3-dB modulation bandwidth (f_{3dB}) is determined by the RC time and the photon lifetime as expressed by $1/(f_{3dB})^2 = (2\pi\tau)^2 + (2\pi RC)^2$, where $\tau = \lambda Q/(2\pi c)$ is the cavity photon lifetime (c is the light speed in vacuum), R is the contact resistance of the electrode, and C is the device capacitance. Since the PZT thin film acts as an insulator, the RC time is minimal, and the high-frequency response is primarily limited by the cavity photon lifetime needed to accumulate and release energy within the ring resonator. To achieve a wider bandwidth, it is advantageous to have a low Q factor ring modulator. However, excessively low Q factor may lead to poor extinction ratios, compromising the quality of high-speed modulation signals. Therefore, careful control of the loss is essential to attain a suitable Q factor. In Figs. 1(d) and 1(e), the calculated

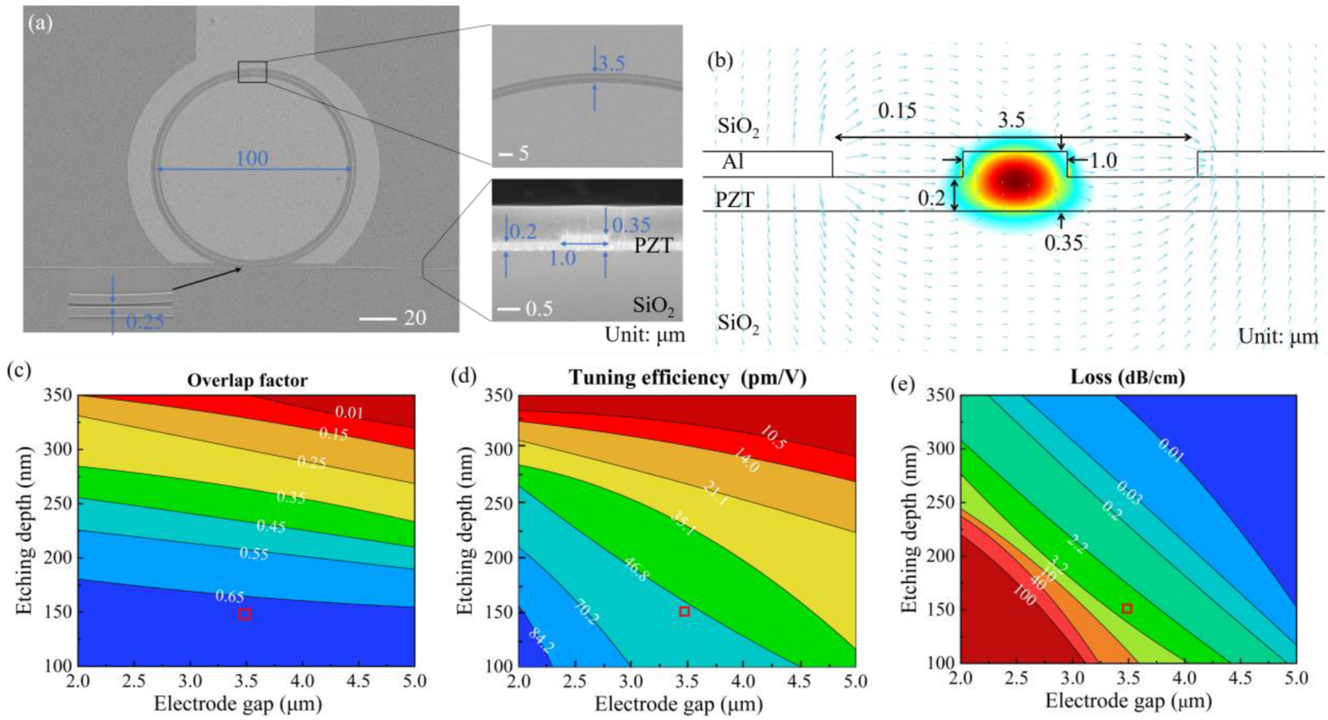

FIG. 1. (a) Top view of a ridge PZT waveguide ring modulator and cross section of the ridge PZT waveguide. (b) Schematic of the ridge PZT waveguide. The fundamental TE optical mode is plotted in false colors. The quiver plot shows the applied electric field distribution between the Al electrodes. (c) Simulation EO overlap factor of the ring modulator. (d) Simulation of the tuning efficiency of the ring modulator. (e) Simulation of the propagation loss. The red rectangles show the approximate parameters used in this work.

tuning efficiency $\Delta\lambda_i/\Delta V$ and loss α_{abs} are plotted as a function of d_e and of g_{inter}, respectively. There is a clear trade-off between $\Delta\lambda_i/\Delta V$ and α_{abs} within the d_e range of 100–350 nm and g_{inter} of 2.0–5.0 µm. By taking into account such a trade-off, we chose etching depth d_e = 150 nm and electrode gap g_{inter} = 3.5 µm to minimize α_{abs} to 2.2 dB/cm (including electrode absorption and waveguide loss) and achieve a high $\Delta\lambda_i/\Delta V$ as 46.8 pm/V.

According to the design above, the PZT ring modulator was fabricated as follows: First, the PZT film was obtained via the chemical solution deposition on a 2-µm silicon dioxide layer sitting on a silicon (from JuheEO).[26] Subsequently, the micro-ring pattern was defined with the metal (Ti+Ni) mask, which was obtained by the electron-beam lithography and lift-off method. The SF_6 plus Ar+ plasma milling method was used to etch the PZT layer for forming the ring resonator. After the metal mask was removed by RCA (NH_4OH, H_2O_2, H_2O mixed by the volume ratio of 1:1:5), the co-planar Al electrodes were deposited via the electron-beam evaporator and lift-off. Finally, the sol-gel SiO_2 top cladding was spin-coated and then baked on a hotplate at 150 °C for 120 min. The PZT thin film has been annealed in the tube at a temperature of 600 °C. Therefore, the handing temperature of 150 °C has no impact on the device. Figure 1(a) illustrates the scanning electron microscope (SEM, Zeiss Gemini500) images of the fabricated modulator. To induce the strong EO effect in PZT thin-film, the ring modulator was poled by applying a DC field of 15 V/μm across the device at room temperature.[17]

III. RESULTS AND DISCUSSIONS

The transmission spectra of the ring resonator were measured by using an end-face coupling system. Light from a tunable laser (TSL-510, Santec) was coupled into the waveguide through a polarization-maintaining fiber. A polarizer located between the laser and the fiber was used to control the input light as TE polarization. The output light from the waveguide was collected by another fiber and then detected via a photodetector (MPM240H, Santec). DC bias voltages from −2 to 10 V generated from a digital source meter (2410, Keithley) were loaded onto the modulator for the $\Delta\lambda_i/\Delta V$ test.

Figure 2(a) shows the measured transmission spectrum of the fabricated ring resonator by scanning the wavelength of the tunable laser. From the measured result, the resonator has a Q factor of ~8000 and an extinction depth of ~13 dB. The $\Delta\lambda_i/\Delta V$ was determined by measuring the spectral shift at one resonant peak as shown in Fig. 2(b). The high-resolution spectra were fitted by the Lorentz function based on the measured points. As can be observed in the spectral change, the extinction ratio varies less than 0.2 dB, and the Q factor almost maintains constant. The resonance wavelength

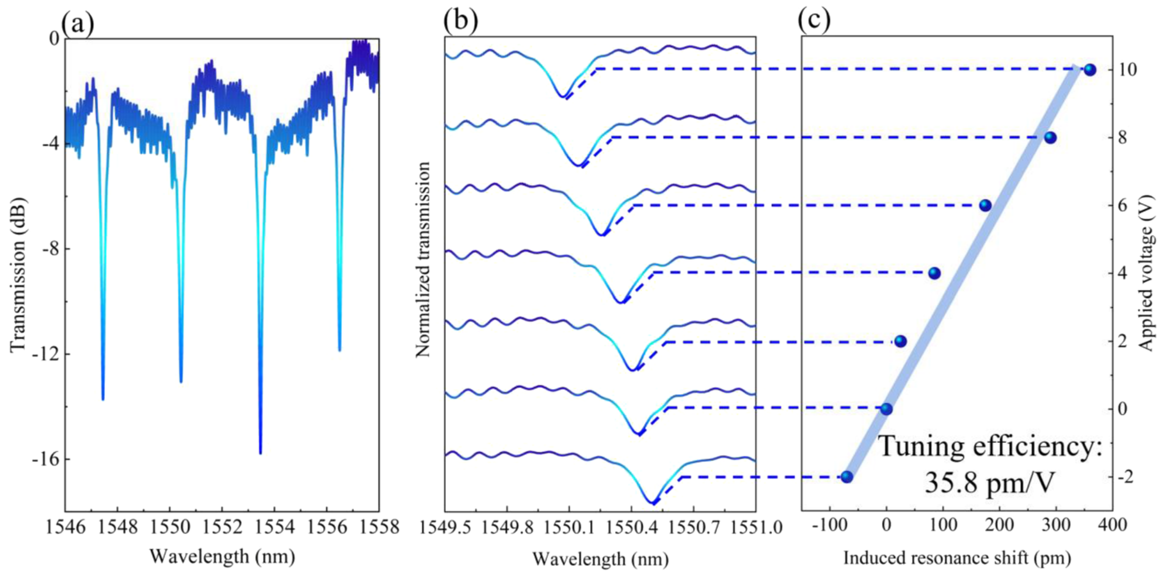

FIG. 2. (a) Normalized transmission spectrum of a PZT ring modulator. (b) Transmission spectra for various DC voltages. (c) Resonance wavelength shift as a function of voltage.

shift is plotted as a function of voltage, and the linear regression as shown in Fig. 2(c) provides a $\Delta\lambda_i/\Delta V$ of 0.0358 nm/V. From this, the half-wave voltage–length product was estimated to be $V_\pi L = |L\lambda_{FSR}V/(2\Delta\lambda_i)| = 1.17$ V·cm, where L is 281 μm and λ_{FSR} is 3 nm. Based on $\Delta\lambda_i/\Delta V$, we calculated the in-device EO coefficient of 100 pm/V in the PZT ring modulator.[17]

The high-speed modulation of the modulator was characterized by using the setup as shown in Fig. 3(a). The input laser was fixed at one resonant wavelength. An arbitrary waveform generator (AWG) (N4975A, Keysight) with non-return-to-zero electrical signals and a driver amplifier (83051A, Keysight) were used to drive the device. The peak-to-peak driving voltage V_{p-p} was 3.0 V. The modulated light, after passing an erbium-doped fiber amplifier (EDFA) and a bandpass filter (BPF), was measured by using an optical sampling oscilloscope with a 45-GHz optical bandwidth (N1092, Keysight). Figure 3(b) exhibits the measured optical eye diagrams of 32 and 56 Gbit/s with clear eye openings. Extinction ratios of these eye diagrams were measured to be ~5.8 and ~3.1 dB. The calculated bandwidth is 24.9 GHz, and the bandwidth can be improved by taking the detuning wavelength method.[27] The modulation speed was limited by the AWG (25 GHz bandwidth), rather than by the PZT ring modulator itself.

As presented above, the ring modulator on the PZTOI platform demonstrated here can achieve high tuning efficiency and high speed. The PZT thin film can be fabricated on a SiO_2/Si substrate by the chemical solution method. The manufacturing procedure is highly scalable and low cost. Meanwhile, the PZT thin film has a large EO coefficient and a wide transparent window. In the past years, researchers found that ferroelectric thin film such as lithium niobate is a kind of excellent material for high-speed modulators due to the strong Pockels effect. Thus,the PZT thin film with a larger EO coefficient was gradually used in modulators when higher-performance devices were needed. In the future, the PZT thin film can also be extended on quartz substrates or heterogeneously integrated with SOI (silicon on insulator) substrates. Therefore, the PZT photonics platform potentially provides a new generation of compact, high-speed, and high bandwidth active devices for telecommunications or other fields (see Note 1 of the supplementary material).

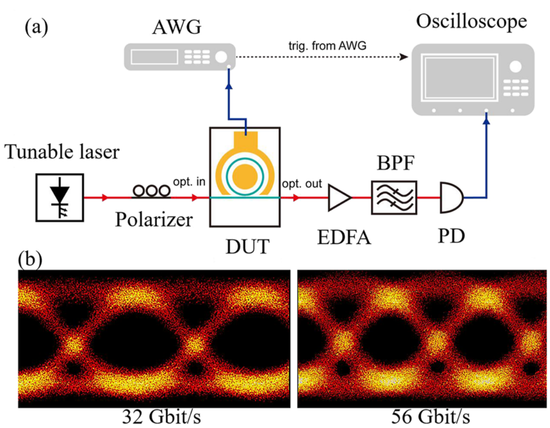

FIG. 3. (a) Sketch of the setup used for the eye diagram measurements. (b) Eye diagrams of a PZT ring modulator, measured with a non-return-to-zero scheme ($2^{11} - 1$ pseudorandom binary sequence) and a peak-to-peak drive voltage of 3.0 V.

TABLE I. Comparison of several performance metrics for EO ferroelectric thin-film ring modulators.

	Propagation loss (dB/cm)	In-device EO coefficient (pm/V)	EO tunability (nm/V)	High-speed modulation (Gbps)
Ridge LN[13]	3.0	30	0.007	40
LN/Si[22]	NA	30	0.0033	9
LN/SiN[28]	0.2	30	0.0029	NA
BTO/SiN[18]	5.6	200	0.0043	20
BTO/Si[20]	10	342	0.04	40
PZT/SiN[17]	1.0	61	0.0134	40
This work Ridge PZT	1.5	100	0.0358	56

Table I lists and compares several modulator metrics of our device with prior demonstrations, focusing on the EO ferroelectric thin-film modulators. In this discussion, we restricted ourselves to ring resonator structures.

Among them, our PZT offers an advantage of a large EO coefficient over LN, so a higher EO tunability $\Delta\lambda_i/\Delta V$ and a lower V_{p-p} can be realized. Further optimization of the structure of waveguide and electrodes could further reduce the electrical signal loss, thus lowering the device energy consumption and facilitating the integration with CMOS circuits. In comparison with BTO, although the PZT modulator presented in this work has no clear advantage in terms of EO tunability $\Delta\lambda_i/\Delta V$, it features much lower propagation loss (measured by the cut-back method,[29] see Note 2 of the supplementary material), indicating a promising potential of being applied in large-scale integrated photonics. The waveguide loss can generally be attributed to two factors: material absorption loss and scattering loss. First, we should prepare crack-free PZT films to minimize material-related losses. Second, we ought to achieve a smooth and contaminant-free waveguide sidewall by optimizing the etching process. More importantly, its modulation speed can achieve up to 56 Gbit/s.

IV. CONCLUSION

To conclude, we have demonstrated an efficient, high-speed, nanophotonic EO ring modulator on the "PZTOI" platform. The PZT thin film was deposited on a SiO_2/Si substrate by using chemical solution deposition. The ridge PZT waveguides enable a strong EO overlap, featuring an ultra-high tuning efficiency of 35.8 pm/V, corresponding to $V_\pi L$ of 1.17 V·cm. Meanwhile, the device exhibited a clear eye diagram of 56 Gbit/s. Together, these results show the suitability of these devices for the on-chip applications. Although we only demonstrated C-band operation in this work, this platform may also be employed into the visible wavelength range.[30,31] We believe that the significantly improved EO modulation performance in "EO ferroelectric thin-film on insulator" will lead to a paradigm shift for ultra-high speed optical communication.

SUPPLEMENTARY MATERIAL

The supplementary material contains the simulation bandwidth results of the Mach–Zehnder modulator on the PZTOI platform and the PZT waveguide loss results.

ACKNOWLEDGMENTS

This work was supported by the National Natural Science Foundation of China (Grant No. 62075184), Project funded by China Postdoctoral Science Foundation (Grant No. 2023M740876), and Zhejiang Province Postdoctoral Research Project (Grant No. ZJ2023103). The authors acknowledge Westlake Center for Micro/Nano Fabrication for the facility support and technical assistance.

AUTHOR DECLARATIONS

Conflict of Interest

The authors have no conflicts to disclose.

Author Contributions

Guolei Liu: Conceptualization (lead); Data curation (lead); Formal analysis (lead); Writing – original draft (equal); Writing – review & editing (equal). **Hongyan Yu**: Data curation (lead); Funding acquisition (equal); Formal analysis (equal); Writing – original draft (equal); Writing – review & editing (equal). **Dasai Ban**: Data curation (equal); Formal analysis (equal). **Bin Li**: Conceptualization (equal); Writing – review & editing (supporting). **Guoqiang Wei**: Software (supporting); Writing – review & editing (supporting). **Chen Yang**: Formal analysis (supporting); Writing – review & editing (supporting). **Jungan Wang**: Formal analysis (supporting); Investigation (equal). **Young-Ik Sohn**: Writing – review & editing (equal); Formal analysis (equal). **Han Yu**: Project administration (equal); Writing – review & editing (equal). **Feng Qiu**: Conceptualization (supporting); Formal analysis (supporting); Funding acquisition (lead); Project administration (lead); Writing – review & editing (equal).

DATA AVAILABILITY

The data that support the findings of this study are available from the corresponding author upon reasonable request.

REFERENCES

[1] S. Ummethala, T. Harter, K. Koehnle, Z. Li, S. Muehlbrandt, Y. Kutuvantavida, J. Kemal, P. Marin-Palomo, J. Schaefer, A. Tessmann, S. K. Garlapati, A. Bacher, L. Hahn, M. Walther, T. Zwick, S. Randel, W. Freude, and C. Koos, "THz-to-optical conversion in wireless communications using an ultra-broadband plasmonic modulator," Nat. Photonics **13**(8), 519–524 (2019).

[2] M. Makarenko, Q. Wang, A. Burguete-Lopez, and A. Fratalocchi, "Photonic optical accelerators: The future engine for the era of modern AI?," APL Photonics **8**(11), 110902 (2023).

[3] G. T. Reed, G. Mashanovich, F. Y. Gardes, and D. J. Thomson, "Silicon optical modulators," Nat. Photonics **4**(8), 518–526 (2010).

[4] C. Haffner, W. Heni, Y. Fedoryshyn, J. Niegemann, A. Melikyan, D. L. Elder, B. Baeuerle, Y. Salamin, A. Josten, U. Koch, C. Hoessbacher, F. Ducry, L. Juchli, A. Emboras, D. Hillerkuss, M. Kohl, L. R. Dalton, C. Hafner, and J. Leuthold, "All-plasmonic Mach–Zehnder modulator enabling optical high-speed communication at the microscale," Nat. Photonics **9**(8), 525–528 (2015).

[5] F. Qiu and Y. Han, "Electro-optic polymer ring resonator modulators [Invited]," Chin. Opt. Lett. **19**(4), 041301 (2021).

[6] Y. Zhang, H. Zhang, J. Zhang, J. Liu, L. Wang, D. Chen, N. Chi, X. Xiao, and S. Yu, "240 Gb/s optical transmission based on an ultrafast silicon microring modulator," Photonics Res. **10**(4), 1127–1133 (2022).

[7] M. He, M. Xu, Y. Ren, J. Jian, Z. Ruan, Y. Xu, S. Gao, S. Sun, X. Wen, L. Zhou, L. Liu, C. Guo, H. Chen, S. Yu, L. Liu, and X. Cai, "High-performance hybrid silicon and lithium niobate Mach–Zehnder modulators for 100 Gbit s^{-1} and beyond," Nat. Photonics **13**(5), 359–364 (2019).

[8] W. Bogaerts, P. De Heyn, T. Van Vaerenbergh, K. De Vos, S. Kumar Selvaraja *et al.*, "Silicon microring resonators," Laser Photonics Rev. **6**(1), 47–73 (2012).

[9] C. T. Phare, Y.-H. Daniel Lee, J. Cardenas, and M. Lipson, "Graphene electro-optic modulator with 30 GHz bandwidth," Nat. Photonics **9**(8), 511–514 (2015).

[10] F. Qiu, A. M. Spring, J. Hong, H. Miura, T. Kashino, T. Kikuchi, M. Ozawa, H. Nawata, K. Odoi, and S. Yokoyama, "Electro-optic polymer ring resonator modulator on a flat silicon-on-insulator," Laser Photonics Rev. **11**(6), 1700061 (2017).

[11] Y. Jo, C. Mai, S. Lischke, L. Zimmermann, and W.-Y. Choi, "Modulation linearity characterization of Si ring modulators," J. Lightwave Technol. **39**(24), 7842–7849 (2021).

[12] C. Haffner, D. Chelladurai, Y. Fedoryshyn, A. Josten, B. Baeuerle, W. Heni, T. Watanabe, T. Cui, B. Cheng, S. Saha, D. L. Elder, L. R. Dalton, A. Boltasseva, V. M. Shalaev, N. Kinsey, and J. Leuthold, "Low-loss plasmon-assisted electro-optic modulator," Nature **556**(7702), 483–486 (2018).

[13] C. Wang, M. Zhang, B. Stern, M. Lipson, and M. Lončar, "Nanophotonic lithium niobate electro-optic modulators," Opt. Express **26**(2), 1547–1555 (2018).

[14] D. W. U. Chan, X. Wu, C. Lu, A. P. T. Lau, and H. K. Tsang, "Efficient 330-Gb/s PAM-8 modulation using silicon microring modulators," Opt. Lett. **48**(4), 1036–1039 (2023).

[15] Y. Enami, A. Seki, S. Masuda, T. Joichi, J. Luo, and A. K. Y. Jen, "Bandwidth optimization for Mach–Zehnder polymer/sol–gel modulators," J. Lightwave Technol. **36**(18), 4181–4189 (2018).

[16] C. Wang, M. Zhang, X. Chen, M. Bertrand, A. Shams-Ansari, S. Chandrasekhar, P. Winzer, and M. Lončar, "Integrated lithium niobate electro-optic modulators operating at CMOS-compatible voltages," Nature **562**(7725), 101–104 (2018).

[17] K. Alexander, J. P. George, J. Verbist, K. Neyts, B. Kuyken, D. Van Thourhout, and J. Beeckman, "Nanophotonic Pockels modulators on a silicon nitride platform," Nat. Commun. **9**(1), 3444 (2018).

[18] F. Eltes, G. E. Villarreal-Garcia, D. Caimi, H. Siegwart, A. A. Gentile, A. Hart, P. Stark, G. D. Marshall, M. G. Thompson, J. Barreto, J. Fompeyrine, and S. Abel, "An integrated optical modulator operating at cryogenic temperatures," Nat. Mater. **19**(11), 1164–1168 (2020).

[19] M. Zhang, C. Wang, P. Kharel, D. Zhu, and M. Lončar, "Integrated lithium niobate electro-optic modulators: When performance meets scalability," Optica **8**(5), 652 (2021).

[20] S. Abel, F. Eltes, J. E. Ortmann, A. Messner, P. Castera, T. Wagner, D. Urbonas, A. Rosa, A. M. Gutierrez, D. Tulli, P. Ma, B. Baeuerle, A. Josten, W. Heni, D. Caimi, L. Czornomaz, A. A. Demkov, J. Leuthold, P. Sanchis, and J. Fompeyrine, "Large Pockels effect in micro- and nanostructured barium titanate integrated on silicon," Nat. Mater. **18**(1), 42–47 (2019).

[21] L. Chen, J. Chen, J. Nagy, and R. M. Reano, "Highly linear ring modulator from hybrid silicon and lithium niobate," Opt. Express **23**(10), 13255–13264 (2015).

[22] L. Chen, Q. Xu, M. G. Wood, and R. M. Reano, "Hybrid silicon and lithium niobate electro-optical ring modulator," Optica **1**(2), 112–118 (2014).

[23] J. E. Ortmann, F. Eltes, D. Caimi, N. Meier, A. A. Demkov, L. Czornomaz, J. Fompeyrine, and S. Abel, "Ultra-low-power tuning in hybrid barium titanate–silicon nitride electro-optic devices on silicon," ACS Photonics **6**(11), 2677–2684 (2019).

[24] D. Ban, G. Liu, H. Yu, X. Sun, N. Deng, and F. Qiu, "High electro-optic coefficient lead zirconate titanate films toward low-power and compact modulators," Opt. Mater. Express **11**(6), 1733–1741 (2021).

[25] D. Ban, G. Liu, H. Yu, Y. Wu, and F. Qiu, "Low driving voltage and low optical loss electro-optic modulators based on lead zirconate titanate thin film on silicon substrate," J. Lightwave Technol. **40**(9), 2939–2943 (2022).

[26] See www.eomaterials.com for information about PZT wafers.

[27] J. Müller, F. Merget, S. Azadeh, J. Hauck, S. R. García, B. Shen, and J. Witzens, "Optical peaking enhancement in high-speed ring modulators," Sci. Rep. **4**, 6310 (2014).

[28] A. N. R. Ahmed, S. Shi, M. Zablocki, P. Yao, and D. W. Prather, "Tunable hybrid silicon nitride and thin-film lithium niobate electro-optic microresonator," Opt. Lett. **44**(3), 618–621 (2019).

[29] F. Qiu, H. Sato, A. M. Spring, D. Maeda, M.-a. Ozawa, K. Odoi, I. Aoki, A. Otomo, and S. Yokoyama, "Ultra-thin silicon/electro-optic polymer hybrid waveguide modulators," Appl. Phys. Lett. **107**(12), 123302 (2015).

[30] W. Gu, Y. Song, J. Liu, and F. Wang, "Lanthanum-based compounds: Electronic band-gap-dependent electrocatalytic materials for oxygen reduction reaction," Chem. - Eur. J. **23**(42), 10126–10132 (2017).

[31] S. K. Pandey, A. R. James, R. Raman, S. N. Chatterjee, A. Goyal, C. Prakash, and T. C. Goel, "Structural, ferroelectric and optical properties of PZT thin films," Physica B **369**(1–4), 135–142 (2005).